and Gamma-Ray Spectroscopy, edited by K. Siegbahn (North-Holland, Amsterdam, 1966), Vol. II, p. 997.

[15]A complete discussion on the various definitions of δ found in the literature, definitions which differ from one another in sign, is given in H. J. Rose and D. M. Brink,

Rev. Mod. Phys. **39**, 306 (1967). The values of δ used in the present work were calculated according to formulas given in the above-mentioned reference, p. 328. The sign convention was modified, however, when necessary to conform to the sign convention of Ref. 14.

Stark Broadening of H_β, H_γ, and H_δ : A Comparison of Theory and Experiment[*]

R. A. Hill and J. B. Gerardo
Sandia Laboratories, Albuquerque, New Mexico 87115

and

Paul C. Kepple[†]
Department of Physics and Astronomy, University of Maryland, College Park, Maryland 20742
(Received 24 April 1970)

A precision comparison is made between the Stark-broadened profiles of H_β, H_γ, and H_δ measured by Hill and Gerardo and the theoretical profiles calculated by Kepple and Griem. In addition, the effects of inelastic collisions between perturbing electrons and the radiating atom are investigated. It is found that the inclusion of the inelastic collisions improves the qualitative agreement between theory and experiment near the line center, but that the Gaunt factors used to estimate the broadening strength of the inelastic collisions overestimate the effect. In terms of half-widths, the best comparison to experiment was obtained using theoretical profiles which omitted inelastic collisions. The electron densities determined from these profiles are 2, 3, and 6% less than the interferometeric values for H_β, H_γ, and H_δ, respectively.

I. INTRODUCTION

When Hill and Gerardo[1] published the results of their measurements of the Stark-broadened profiles of the lines H_β, H_γ, and H_δ, the best theoretical profiles available for comparison were those of Griem, Kolb, and Shen[2,3] (GKS I, II). When Kepple and Griem[4] (KG) published their theoretical profiles, they compared the half-intensity widths of their profiles to the GKS I, II profiles and thus formed only an indirect comparison to experiment. In this paper, these experimental and theoretical line shapes are compared in detail.

One of the difficulties (source of errors) in comparisons between experiment and theory is that the theoretical profiles are usually calculated for some set of temperatures and densities which seldom coincide with the actual temperature and density of the experiment. Thus, one must interpolate in the tables of computed profiles. In the case where the shape of the profile does not change much with temperature and density (H_β, for example), the interpolation is easy and resultant errors small. However, when the shape of the line changes noticeably with temperature or density (as in the case of H_γ) then one must be more careful or significant errors will be introduced by the interpolation. In order to avoid these errors, the computed code for Stark-broadened hydrogen lines (described briefly in KG, and in more detail in Ref. 5) was

rerun for the electron temperatures and electron densities of the experiment. The only difference between the code as described in Ref. 5 and that used here is the inclusion of contributions to the line broadening from inelastic collisions between perturbing electrons and radiating atoms as described in Sec. II. The results of the comparison of KG theory (both with and without the contributions due to inelastic collisions) with experiment appears in Sec. III.

II. INELASTIC COLLISIONS

The matrix representation of the electron broadening operator contains terms of the sort

$$\sum_{\sigma\gamma} G(n_\alpha, n_\gamma) \langle \alpha' | R_\sigma | \gamma \rangle \langle \gamma | R_\sigma | \alpha'' \rangle ,$$

where α', α'', and γ represent complete sets of quantum numbers (n, l_1, l_2, m) and R_σ is a component of the electron position operator (in atomic units). For the elastic terms ($n_\alpha = n_\gamma$), G reduces to the $\overline{G}$ of KG. Since these elastic terms are by far the largest, the inelastic terms ($n_\alpha \neq n_\gamma$) were simply omitted in GKS I, II, and KG. To investigate the change in the line shape introduced by this omission of inelastic terms, the quantity G (for $n_\alpha \neq n_\gamma$) is replaced by a semiempirical Gaunt factor.[6] With the inelastic collision thus accounted for, the electron broadening operator is

$$\langle \alpha' | \langle \beta' | \varphi_{ab} | \alpha'' \rangle | \beta'' \rangle = \delta_{\beta'\beta''} \left[\bar{G} \sum_{\sigma\alpha} \langle \alpha' | R_{a\sigma} | \alpha \rangle \langle \alpha | R_{a\sigma} | \alpha'' \rangle + \left(\sum_{\substack{\sigma\gamma \\ n_\gamma \neq n_\alpha}} \frac{\pi}{\sqrt{3}} \langle \bar{g}(\Delta E_{n_\alpha, n_\gamma}) \rangle_{av} \langle \alpha' | R_{a\sigma} | \gamma \rangle \langle \gamma | R_{a\sigma} | \alpha'' \rangle \right) \right]$$

$$+ \delta_{\alpha'\alpha''} \left[\bar{G} \sum_{\sigma\beta} \langle \beta' | R_{b\sigma} | \beta \rangle \langle \beta | R_{b\sigma} | \beta'' \rangle + \left(\sum_{\substack{\sigma\gamma \\ n_\gamma \neq n_\beta}} \frac{\pi}{\sqrt{3}} \langle \bar{g}(\Delta E_{n_\beta, n_\gamma}) \rangle_{av} \langle \beta' | R_{b\sigma} | \gamma \rangle \langle \gamma | R_{b\sigma} | \beta'' \rangle \right) \right]$$

$$- 2\bar{G} \sum_\sigma \langle \alpha' | R_{a\sigma} | \alpha'' \rangle \langle \beta' | R_{b\sigma} | \beta'' \rangle \, ,$$

where $\langle \bar{g}(\Delta E) \rangle_{av}$ is the thermal average of a semi-empirical Gaunt factor,[7] and $\Delta E_{n,n'}$ is the difference in energy levels between hydrogenic states with principal quantum numbers n and n'. Since the matrix elements decrease rapidly with Δn, those elements on or near the diagonal can be approximated by the term with $\Delta n = 1$, with an error less than 40% (less than 30% when the Gaunt factors are included). The relative error incurred by using the $\Delta n = 1$ terms for the elements further off the diagonal is quite large, however, since these off-diagonal terms are much smaller than the near-diagonal terms, the actual error (the error in the electron contribution to the profile) is negligible. Thus, since the entire inelastic contribution is small, all terms except the term with $n_\gamma = n_\alpha(n_\beta)$ + 1 were neglected. The effect on the individual line shapes of adding the contributions due to inelastic collisions will be discussed in Sec. III.

III. COMPARISON OF THEORY AND EXPERIMENT

The comparison of theory and experiment was carried out using H_β, H_γ, and H_δ profiles which were recorded in an earlier experiment.[1] High-accuracy measurements were obtained by using a rapid-scan spectrometer to record the Stark-broadened line profiles,[8,9] multiple-pass laser interferometers ($\lambda_1 = 1.1523 \ \mu$ and $\lambda_2 = 0.6328 \ \mu$) to

independently measure the electron density,[10,11] and a long uniform plasma source in order to minimize boundary-layer effects. A complete description of the experiment is given in Ref. 1. For this comparison of theory and experiment, the theoretical profiles were computed for the particular values of electron density and temperature measured in the experiment. These theoretical profiles were modified by the measured instrument function (including Doppler broadening as described in Ref. 1).

The electron temperature was determined from the H_β-to-continuum ratio; an example of the data from which this ratio was obtained is shown in Fig. 1. The interferometric value of electron density for this particular record is $2.75 \times 10^{16} \ cm^{-3}$. The blue wing is shown in Fig. 1(b); the red wing and central portion of the H_β profile (recorded at one-fourth the sensitivity) are shown in Fig. 1(a). The large and small dashed lines represent the continuum intensity at the increased and decreased sensitivity, respectively. The intensity ratio of H_β to 100 Å of continuum is 24.4 which corresponds to $T_e = 21\,000 \ ^\circ K$.[12] The half-intensity width of a profile calculated without corrections for inelastic collisions (IC) for an electron density of $2.75 \times 10^{16} \ cm^{-3}$ including finite slit width and rise-time effects is 20.5 Å in good agreement with the measured value of 20.4 Å.
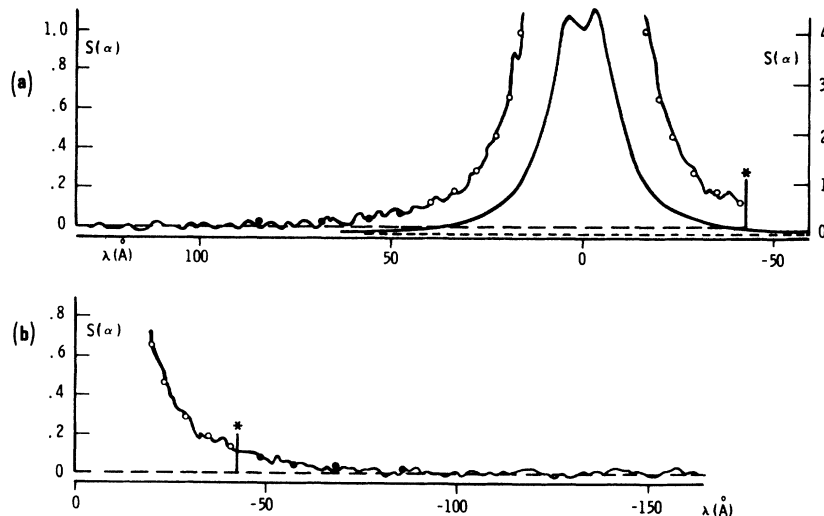

FIG. 1. Example of an H_β profile and the adjoining continuum intensity recorded at $N_e = 2.75 \times 10^{16} \ cm^{-3}$. The red wing and central portion of the H_β profile (at one-fourth the sensitivity) are shown in (a); the blue wing is shown in (b). The intensity ratio of H_β to 100 Å of continuum is 24.4 which corresponds to $T_e = 21\,000 \ ^\circ K$.

In order to determine whether the underlying in-
tensity is correctly assigned to background radia-
tion, a comparison of the theoretical and observed
line wings was carried out. The theoretical inten-
sities at a number of discrete wavelengths were
calculated without IC for $N_e = 2.75 \times 10^{16}$ and T_e
$= 21\,000$ °K. These intensities are plotted with small
circles in Fig. 1. In addition, theoretical inten-
sities were calculated with the asymptotic expres-
sion[4]

$$S_{as} = (3.57 \times 10^{-3}/\alpha^{5/2})[1.90 + 0.70(0.35/\alpha)^{3/2}],$$

where α is the reduced wavelength. These inten-
sities are plotted with dots in Fig. 1. The standard
deviation between the experimental line-wing in-
tensities and the calculated intensities is 5.7%.
This agreement indicates that the method used to
separate the underlying continuum is adequate and
the H_β-to-continuum ratio should give a meaningful
temperature measurement.

In the previous analysis of the H_β profiles,[1] the
half-intensity widths of the experimental profiles
were found to be in excellent agreement with the
half-intensity widths of the theoretical profiles as
calculated by GKS II. As shown in Fig. 2, the new
KG theoretical profiles are somewhat broader than
the GKS II profiles, with the result that the agree-
ment between theory and experiment is not as good
with the KG profiles. A comparison between a pro-
file that was recorded at $N_e = 2.78 \times 10^{16}$ cm^{-3} and
KG theoretical profiles (including modification by
the instrument function) is shown in Fig. 3. The
comparison with the theoretical profile without IC
is obviously better than that which includes IC;
however, the half-intensity widths in both cases are
within 5% of the experimental value. The compar-
ison between theory and experiment is somewhat
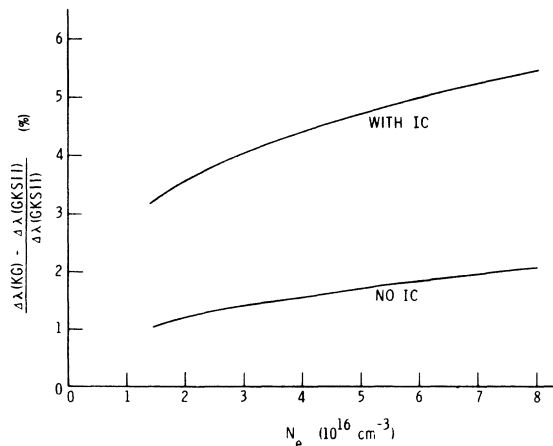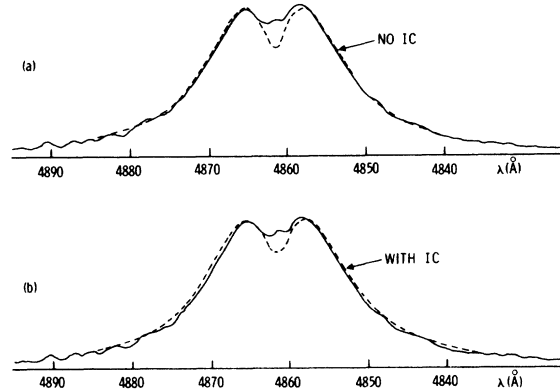better at the line center with IC than without IC,

FIG. 3. Comparison of an observed profile for
$N_e = 2.78 \times 10^{16}$ cm^{-3} (solid line) with theoretical profiles
which have been modified by the instrument functions.
Calculated profiles in (a) are without inelastic collisions
and in (b) include the inelastic collisions. Narrow band
at the bottom represents the continuum intensity for
$T = 21\,000$ °K.

i.e., the central intensity minimum is not as deep
if the IC are included. Even in the latter case,
however, the agreement is not satisfactory. The
excess radiation at the line center may be caused
by H_β line radiation from the cold gas in the bound-
ary layer at the end window. This radiation would
be concentrated at the line center due to the low
electron density in the boundary layer. On the oth-
er hand, the calculations do not include the ion dy-
namics corrections[13] to the (ion) quasistatic broad-
ening (the correction to the ion quasistatic broad-
ening due to the relative motion between the ions
and radiating atom) which may be non-negligible
under some conditions of interest. One may ex-
pect that the inclusion of the ion dynamics correc-
tions into the code for the total line profile will
substantially reduce the dip in the center of the H_β
profile thus improving somewhat the comparison
between experiment and theory.

The comparison between theory and experiment
for electron densities in the range $1.5-7.5 \times 10^{16}$
cm^{-3} is shown in Fig. 4. Each data point represents
the percent difference between the interferometric
value of electron density $N_e(I)$ and the average value
of electron density, as inferred from the half-in-
tensity widths of from 10 to 20 H_β profiles, $N_e(S)$.
The vertical error bars represent the standard
deviation for the average values $N_e(S)$ and do not
include the estimated systematic error. This com-
parison of theory and experiment indicates that the
values of electron density inferred from measured
half-intensity widths using the theoretical profiles
are 4-8% too low when the IC are included and
1-3% too low when they are not. In both cases this
applies for the N_e range $1.5-7.5 \times 10^{16}$ cm^{-3}.

In the previous analysis of the H_γ profiles,[1] the

FIG. 2. Comparison of the half-intensity widths of
GKS II H_β profiles with the half-intensity widths of pro-
files calculated with and without inelastic collisions.

TABLE I. Comparison of theoretical linewidths with measured widths for $N_e = 2.60 \times 10^{16}$ cm^{-3}.

Normalized intensity	Width (Å)	Width for $N_e = 2.6 \times 10^{16}$ without IC [a] (Å)	Diff calc − obs (%)	Width for $N_e = 2.36 \times 10^{16}$ with IC [a] (Å)	Diff calc − obs (%)
0.1	61.8 ± 1.1	64.1	3.6	63.0	1.94
0.2	45.1 ± 0.8	45.8	1.5	45.0	−0.22
0.3	36.0 ± 0.5	36.5	1.3	36.0	0.0
0.4	29.6 ± 0.5	29.9	1.0	29.6	0.0
0.5	24.4 ± 0.5	24.1	−1.2	24.3	−0.41
0.6	19.7 ± 0.5	17.9	−10.0	19.1	−3.05
0.7	14.6 ± 0.7	10.0		12.8	
0.8	10.0 ± 1.1	6.0		7.5	
0.9	5.4 ± 0.5	3.6		4.3	

[a] These widths are for theoretical profiles which have been modified by the instrument function.
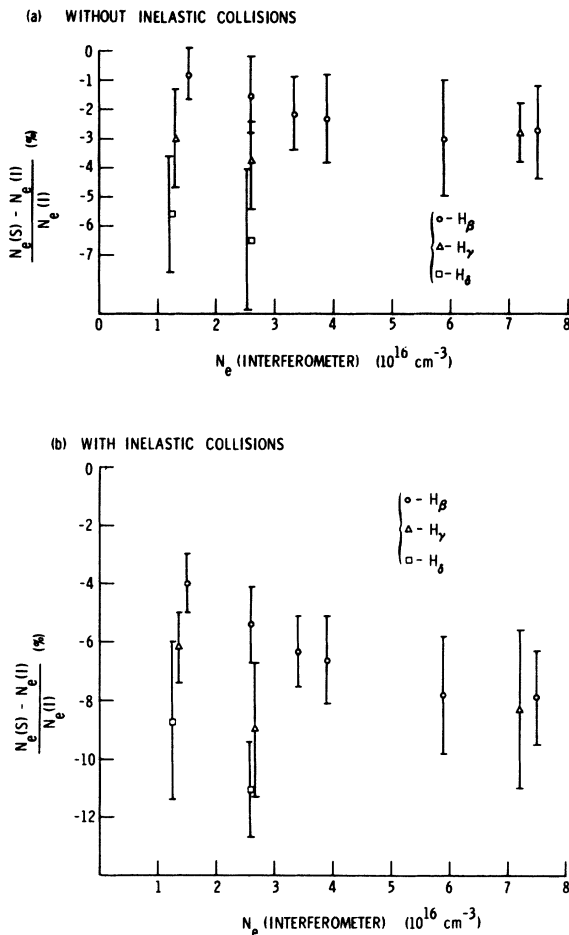

FIG. 4. Over-all comparison between values of electron density N_e (I) as determined by the laser interferometer, and values N_e(S) inferred from Stark-broadened H_β, H_γ, and H_δ profiles using calculated profiles (a) without inelastic collisions and (b) with inelastic collisions. The over-all estimated uncertainty in this comparison is ± 4%. Both comparisons are better than the estimated uncertainties in the calculated profiles (± 10%).

half-intensity widths of the experimental profiles were 11–25% larger than the half-intensity widths of the theoretical profiles as calculated by GKS I for the electron density range $1.3–7.1 \times 10^{16}$ cm^{-3}. Since the new KG theoretical profiles are broader than the GKS I profiles, the agreement between theory and experiment has been improved.

The signal-to-noise ratio for the recorded H_γ line profiles was less than in the case of H_β because of the smaller line-to-continuum ratio. In order to smooth out this "noise" contribution several profiles which were recorded on consecutive discharges were averaged to obtain a new profile which was then analyzed in detail. The background level was established by using the H_γ-to-continuum ratio for an electron temperature of 21 000 °K. The average "fractional-intensity" widths of six such averaged profiles, each representing an electron density of 2.60×10^{16} cm^{-3}, are shown in Table I along with their standard deviations. The analysis of these averaged data was carried out with the aid of the calculated curves of electron density vs fractional-intensity width shown in Fig. 5. These calculated fractional-intensity widths have been modified by the instrument functions. The averaged fractional-intensity widths from Table I are plotted on their respective curves in Fig. 5 where the symbols Δ and x have been used to distinguish the curves with and without IC, respectively. Comparing the averaged fractional-intensity widths with the calculated values without IC at $N_e = 2.60 \times 10^{16}$, the measured (0.1–0.4) fractional-intensity widths are smaller than the calculated widths while the measured (0.5–0.9) fractional-intensity widths are larger than the calculated widths. This comparison is further illustrated in Fig. 6(a) where the observed and calculated profiles are represented by solid and dashed lines, respectively. The percentage difference between the measured and calculated widths are listed in Table I. While the half-intensity widths disagree by only 1.2%, the central core of the calculated profile is
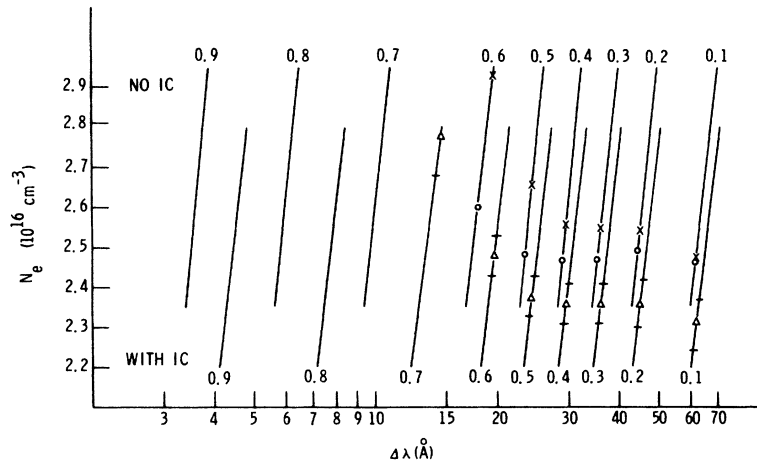
FIG. 5. Calculated curves of electron density vs fractional-intensity width of H_γ profiles for $T_e = 21\,000\,°$K. These widths have been modified by the instrument functions. Averaged fractional-intensity widths for several profiles recorded at $N_e = 2.60 \times 10^{16}$ cm^{-3} are plotted with the symbols (Δ and x) on the curves with and without inelastic collisions, respectively. Circles represent the best fit for the line wings. Error flags represent the standard deviation in the measured widths shown in Table I.

much too narrow. Because of the disagreement at the line center (which again would be reduced by the inclusion of the ion dynamics correction[13]), a second comparison was carried out with the goal of obtaining a good fit in the line wings while disregarding the line center entirely. The results plotted in Fig. 5 (with the symbol o), and further illustrated in Fig. 6(b), show that the line wings of a profile calculated at $N_e = 2.50 \times 10^{16}$ cm^{-3} compare very favorably with the observed line wings if the calculated profile is 5% more intense at the line center than the observed profile. The standard deviation in the (0.1–0.6) fractional-intensity widths for this comparison is 1.4%. Thus, the line wings correspond to an electron density 3.9% less than the value observed with the interferometer.

A comparison was also carried out for the observed profile and calculated profiles which included IC. These results, plotted in Fig. 5 (with the symbol Δ) and further illustrated in Fig. 6(c), show that a profile calculated for $N_e = 2.36 \times 10^{16}$ cm^{-3} compares very favorably with the observed profile. The standard deviation in the 0.1–0.6 fractional-intensity widths, for the differences shown in Table I, is 1.5%. The comparison between the observed and calculated line shapes is much improved at the line center by the inclusion of. IC. In this case, however, the line profile corresponds to an electron density 9.1% less than the interferometric value.

The results of the above comparison and comparisons at 1.3×10^{16} and 7.1×10^{16} cm^{-3} are shown in Figs. 4(a) and 4(b). The comparison in both cases are those obtained by fitting the line wings, i.e., the (0.1–0.6) fractional-intensity widths as discussed above. The error bars are the standard deviations in the widths multiplied by 1.5, a factor which is due to the fact that $N_e \sim \Delta\lambda^{3/2}$, where $\Delta\lambda$ is the half-intensity width. This comparison of theory and experiment indicates that the values of

electron density inferred from the line wings using the theoretical profiles with and without IC are ~ 8% and ~ 3% too low, respectively.

In the previous analysis of the H_δ profiles,[1] the half-intensity widths of the experimental profiles were 7% smaller than the half-intensity widths of the theoretical profiles as calculated by GKS I for the electron-density range $1.3–2.8 \times 10^{16}$ cm^{-3}.
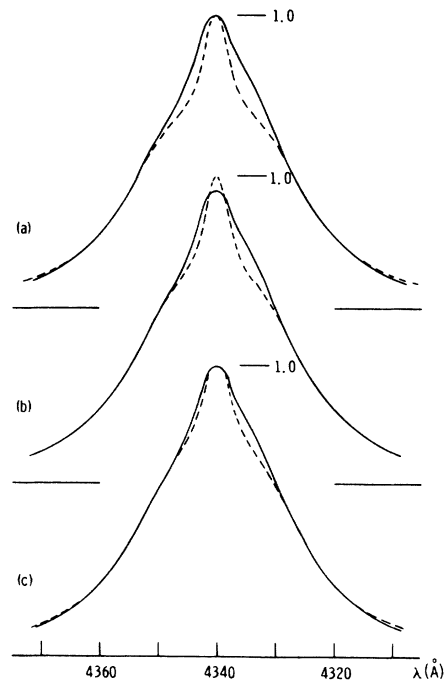

FIG. 6. Comparison of an averaged H_γ profile ($N_e = 2.60 \times 10^{16}$ cm^{-3}, solid line) and calculated profiles (dashed line) for (a) $N_e = 2.60 \times 10^{16}$ cm^{-3} without inelastic collisions, (b) $N_e = 2.50 \times 10^{16}$ cm^{-3} without inelastic collisions, and (c) $N_e = 2.36 \times 10^{16}$ with inelastic collisions. The effect of the inelastic collisions is particularly noticeable near the line center.

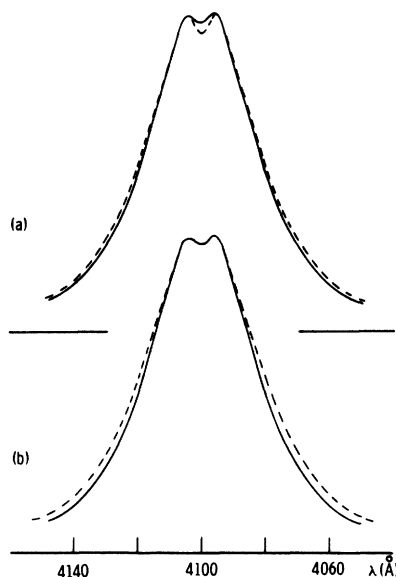FIG. 7. Comparison of an averaged H_δ profile
$(N_e = 2.60 \times 10^{16}$ cm^{-3}, solid line) and calculated profiles
(dashed lines) for $N_e = 2.60 \times 10^{16}$ cm^{-3} (a) without inelas-
tic collisions and (b) with inelastic collisions.

Since the new theoretical profiles are slightly broad-
er than the GKS I profiles, the agreement between
theory and experiment is somewhat worse.

As in the case of H_γ, several H_δ profiles which
were recorded on consecutive discharges were av-
eraged in order to smooth out the contribution due
to the continuum. The background level was de-
termined by using the H_δ-to-continuum ratio for an
electron temperature of 21 000 °K. An averaged
"observed" profile for an electron density of 2.60
$\times 10^{16}$ cm^{-3} is shown with a solid line in Fig. 7.
The blue wing of this averaged profile has been re-
duced in intensity to compensate for the contribu-
tion of the red wing of H_ϵ. For $N_e = 2.60 \times 10^{16}$cm^{-3}

and $T_e = 21\ 000$ °K, the theoretical H_ϵ profile has
full half-intensity and tenth-intensity widths of 51.9
and 134.6 Å, respectively. Theoretical H_δ profiles
calculated for $N_e = 2.60 \times 10^{16}$ cm^{-3} and modified by
the instrument functions are shown with dashed
lines in Fig. 7. The half-intensity widths of the
profiles calculated without IC [Fig. 7(a)] and with
IC [Fig. 7(b)] are 4.5 and 7.5% larger than the ob-
served value, respectively. As in the example of
H_β, the central intensity minimum of the calculated
profiles is less if IC are included which is in better
agreement with observation.

As in the example of H_γ, the analysis of the H_δ
profiles was carried out with the aid of the calcu-
lated curves of electron density vs fractional-in-
tensity width shown in Fig. 8. These curves have
been modified by the instrument functions. The
measured fractional-intensity widths are plotted on
their respective curves where the symbols Δ and x
have been used to distinguish curves with and with-
out IC, respectively. An analysis of this data in-
dicates that the observed profile compares favor-
ably with a profile calculated for $N_e = 2.43 \times 10^{16}$
cm^{-3} without IC and for $N_e = 2.31 \times 10^{16}$ cm^{-3} with
IC. The standard deviation in the (0.1–0.9) frac-
tional-intensity widths for this comparison is 1.9%
without IC and 1.1% with IC. Thus, the observed
profile corresponds to an electron density 11.1 and
6.5% less than the value observed with the inter-
ferometer for the calculations with and without IC,
respectively.

The results of the above comparison and a simi-
lar comparison at 1.3×10^{16} cm^{-3} are shown in Figs.
4(a) and 4(b). The error bars represent the standard
deviations in the widths multiplied by 1.5 as in the
example of H_γ.

IV. DISCUSSION

The over-all comparison between theory and ex-
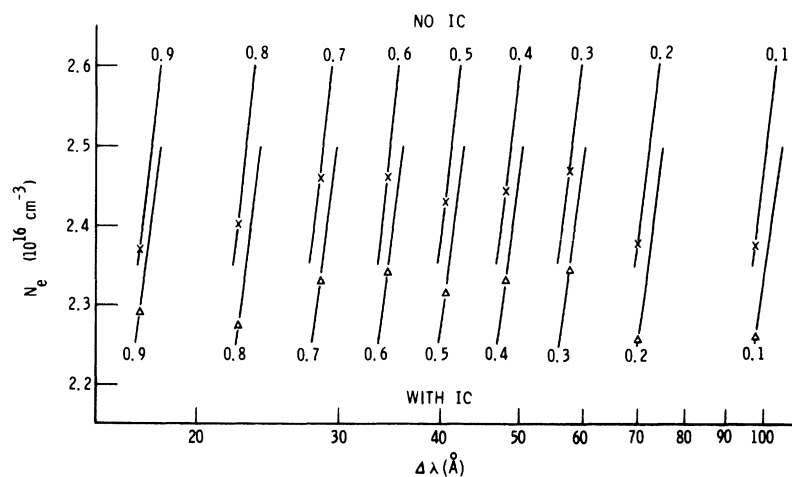periment, shown in Fig. 4, indicates that values of

FIG. 8. Calculated curves of elec-
tron density vs fractional-intensity
width of H_δ profiles for $T_e = 21\ 000$°K.
These widths have been modified by
the instrument functions. The av-
eraged fractional-intensity widths
for the profile shown in Fig. 7 are
plotted with the symbols (Δ and x)
on the curves with and without in-
elastic collisions, respectively.

electron density determined from the theoretical profiles without IC are about 2, 3, and 6% less than the interferometric values for H_β, H_γ, and H_δ, respectively. The values of electron density determined from theoretical profiles with IC are about 6, 8, and 10% less than the interferometric values for H_β, H_γ, and H_δ, respectively. The over-all estimated uncertainty in this comparison is ± 4%: ± 2% in establishing an average value for the electron density as previously discussed,[1] and ± 2% in analyzing the line profiles. While both of the above comparisons are better than the estimated uncertainties in the calculated profiles (± 10%), the profiles with the IC are somewhat too broad, even though these corrections certainly improve the comparison in the line cores. Thus, it appears than when the contribution of the inelastic collisions is simply added to that of the elastic, the Gaunt factors overestimate the effect. This is partly due to the fact that the strong collision term already partially accounts for the inelastic collisions. As mentioned before, the inclusion into the code of the ion dynamics correction may improve the comparison near the line center.

It is interesting to note that the experimental line profiles are narrower than predicted by theory, and that this difference between theory and experiment increases as the upper quantum number increases. At an electron density of 2.60×10^{16} cm^{-3}, the (half) half-intensity widths of H_γ, H_δ, and H_ϵ are 11.5, 20.9, and 26.0 Å, respectively, and the (half) tenth-intensity widths are 31.5, 51.5, and 67.3 Å, respectively. Because the $(H_\gamma - H_\delta)$ and $(H_\delta - H_\epsilon)$ line separations are 238.8 and 131.6 Å, respectively, it appears that for these densities, the wings of the Balmer lines are beginning to overlap. Thus, it is reasonable to expect an interaction of the upper-state energy levels which would cause a spectral line narrowing. This effect, which is not included in the present Stark-broadening theory,[14] would increase as the series limit is approached.

In order to compare the results of this experiment with the recently published results of Beng-

ston et al.,[15] it is necessary to compute the ratio of the electron density determined from H_γ to that determined from H_β. The mean ratio of the electron density determined from the H_β profiles to that determined from the interferometer is 0.978 with a mean standard deviation of ± 1.45%. The mean ratio of the electron density determined from the H_γ profiles to that determined from the interferometer is 0.968 with a mean standard deviation of ± 1.47%. Thus, the ratio of the electron density determined from H_γ to that determined from H_β is 0.99 ± 0.02. This value is in satisfactory agreement with the value 1.01 ± 0.02 reported by Bengston et al.

Finally, it is worthwhile to investigate two of the more important experimental parameters and in particular, the magnitude of variation in these parameters necessary to show an improvement in the comparison between theory and experiment. These quantities are the plasma length L and the relative continuum intensity. For the interferometric measurement of electron density, $N_e \propto L^{-1}$, where $L = 14.7$ cm.[1] In order to decrease the interferometric density by 4%, the plasma length L would have to be increased to 15.3 cm, a value longer than the plasma container (14.9 cm). If, on the other hand, the continuum intensity at H_δ were decreased such that the half-intensity width of the observed profile agrees with that for a theoretical profile corresponding to 2.60×10^{16} cm^{-3}, then the H_δ-to-continuum ratio corresponds to an electron temperature of 12 000 °K. This would require an H_β-to-continuum ratio of approximately 70 which would imply that the continuum measurement shown in Fig. 1 is about three times too large. This result is hard to accept in view of the good agreement between the observed and calculated H_β line wings for a temperature of 21 000 °K.

ACKNOWLEDGMENT

---

*Work supported by the U.S. Atomic Energy Commission and the National Aeronautics and Space Administration.

†Present address: U.S. Naval Research Laboratory, Washington, D.C.

[1]R. A. Hill and J. B. Gerardo, Phys. Rev. 162, 45 (1967).

[2]H. R. Griem, A. C. Kolb, and K. Y. Shen, Phys. Rev. 116, 4 (1959).

[3]H. R. Griem, A. C. Kolb, and K. Y. Shen, Astrophys. J. 135, 272 (1962).

[4]P. Kepple and Hans R. Griem, Phys. Rev. 173, 317 (1968).

[5]P. Kepple, University of Maryland, Center for Theoretical Physics Report No. 831 (unpublished).

[6]This approach was suggested by H. Van Regemorter [Astrophys. J. 136, 906 (1967)] and applied by Griem to the case of isolated ion lines [Hans R. Griem, Phys. Rev. 165, 258 (1968)].

[7]We used the numerical values tabulated in C. W. Allen, Astrophysical Quantities, 2nd ed. (The Athelone Press, University of London, London, 1964), p. 43.

[8]R. A. Hill and R. D. Fellerhoff, Appl. Opt. 5, 1105 (1966).

[9]R. A. Hill, Appl. Opt. 7, 2184 (1968).

[10]J. B. Gerardo and J. T. Verdeyen, Proc. IEEE 52, 690 (1964).

[11]J. B. Gerardo, J. T. Verdeyen, and M. A. Gusinow, J. Appl. Phys. 36, 2146 (1965); 36, 3526 (1965).

[12]H. R. Griem, Plasma Spectroscopy (McGraw-Hill,

New York, 1964), p. 281.

[13]H. R. Griem, Comments At. Mol. Phys. 2, 19 (1970);
J. W. Dufty, Phys. Rev. A 2, 534 (1970).

[14]The case of overlapping lines which originate from
all the states of a degenerate level has been included
here; the case of overlapping lines originating from
levels of different principal quantum number has not
been included. While a (practical) theory to treat the
complete profile of overlapping (nondegenerate) lines
does not exist, Baranger's one-electron approximation
[M. Baranger, in *Atomic and Molecular Processes*,
edited by D. R. Bates (Academic, New York, 1962)] can
be used to show the effect of the interference (or over-
lapping) in the line wing. From Baranger's Eq. 122, the
ratio of the interference term to the main term is

$$\frac{(\omega - \omega_{if})^2}{(\omega - \omega_{ij})(\omega - \omega_{i'f})} = \frac{\omega - \omega_{if}}{\omega - \omega_{i'f}},$$

where ω_{if} $(\omega_{i'f})$ is the frequency of the transition from
initial state $i(i')$ to the final state f. It is difficult to
translate this correction, which applies only in the wings,
into a meaningful correction to the half-intensity width;
however, it does have the appropriate qualitative be-
havior. Within a series, the nearest neighbor to a given
line lies at a higher frequency, thus, $\omega_{i'f} > \omega_{if}$. As a
result, the entire line profile corresponding to the transi-
tion $i \rightarrow f$ is shifted to the red. The effect is greater,
however, for $\omega_{if} < \omega < \omega_{i'f}$, than for $\omega < \omega_{if} < \omega_{i'f}$, so that
the line profile should be somewhat compressed. The
magnitude of the correction increases as the principal
quantum number of the initial state increases due to the
decreased spacing between series members, and to the in-
creased broadening of the higher series members.

[15]R. D. Bengston, M. H. Miller, W. D. Davis, and
J. R. Grieg, Astrophys. J. 157, 957 (1969).

Relationship between Unrestricted and Extended Hartree-Fock Wave Functions as Function of Number of Electrons*

F. Martino and J. Ladik†

Physics Department, City College of the City University of New York, New York, New York 10031

The justification of the use of unprojected many-electron wave functions for solids and
large molecules is examined from the point of view of an extended Hartree-Fock method in
the one-λ approximation presented in previous papers. It is shown that, in the limit of a
large number of electrons, the Hartree-Fock operators are the same for the projected and
unprojected case. It is further shown that the expectation value of purely spatial operators
for the projected and unprojected functions are equal in this limit. Graphs of the differences
of the relevant quantities as a function of number of electrons are given.

The question of the relation between the unre-
stricted [different orbitals for different spins
(DODS) without spin projection] and extended
Hartree-Fock (DODS with spin projection before
variation) methods has been of interest both in
molecular and solid-state physics.[1] In the partic-
ular case of the alternant molecular orbital (AMO)
method[2,3] it has been shown that the expectation
value of the total Hamiltonian is the same for the
singlet ground state and the unprojected function if
the number of electrons goes to infinity. In a series
of papers[4] (I–III hereafter) we have formulated an
extended Hartree-Fock (HF) method in the one-λ
approximation[3] both for molecules and solids. This
method provides the possibility of investigating the
above question from a new aspect.

The extended Hartree-Fock self-consistent-field
(SCF) equations are [see (12a) and (12b) of I]:

$$H^\alpha \varphi_i^\alpha + h^\beta \varphi_i^\beta = \epsilon_i^{\alpha\alpha} \varphi_i^\alpha + \epsilon_i^{\alpha\beta} \varphi_i^\beta,$$ (1a)

$$H^\beta \varphi_i^\beta + h^\alpha \varphi_i^\alpha = \epsilon_i^{\beta\beta} \varphi_i^\beta + \epsilon_i^{\alpha\beta} \varphi_i^\alpha.$$ (1b)

Here the operators are

$$H^\alpha = (\Lambda_{0,0}^s)^{-1} \left(\Lambda_{0,1}^s H^N + \sum_{j=1}^n (\Lambda_{0,2}^s (J_j^{\alpha\alpha} - K_j^{\alpha\alpha} + J_j^{\beta\beta}) \right.$$

$$\left. + 2\lambda \Lambda_{1,2}^s \{[J_j^{\alpha\beta}] - [K_j^{\alpha\beta}]\} + \Lambda_{1,2}^s [K_j^{\beta\beta}] \right),$$ (2a)

$$h^\alpha = (\Lambda_{0,0}^s)^{-1} \left(\lambda \Lambda_{1,1}^s H^N + \sum_{j=1}^n (\lambda \Lambda_{1,2}^s (J_j^{\alpha\alpha} + J_j^{\beta\beta} \right.$$

$$\left. - K_j^{\alpha\alpha} - K_j^{\beta\beta}) + \lambda^2 \{\Lambda_{1,2}^s K_j^{\alpha\beta} + \Lambda_{2,2}^s (2[J_j^{\alpha\beta}] - K_j^{\beta\alpha})\}\right),$$ (2b)

$$H^\beta = H^\alpha \ (\alpha \rightarrow \beta), \qquad h^\beta = h^\alpha \ (\alpha \rightarrow \beta),$$

$$[J_j^{\alpha\beta}] = \tfrac{1}{2}(J_j^{\alpha\beta} + J_j^{\beta\alpha}), \quad [K_j^{\alpha\beta}] = \tfrac{1}{2}(K_j^{\alpha\beta} + K_j^{\beta\alpha}).$$ (2c)

The operator H^N is the usual one-electron op-
erator and the generalized $J_j^{\gamma\delta}$ Coulomb, $K_j^{\gamma\delta}$ (γ
$= \alpha$ or β) exchange operators are defined in I [see
Eqs. (10b) and (10c) of I]. The constants $\Lambda_{r,t}^s$ which
contain the effect of spin projection are defined by

$$\Lambda_{r,t}^s = \sum_{k=0}^{n-t} (-1)^{k+r} \binom{n-t}{k} C_n(s, k+r)\lambda^{2k},$$ (3)

where $2n$ is the number of electrons, $2s+1$ is the
multiplicity, the $C_n(s, k+r)$ are the Sanibel coeffi-
cients,[5] and finally

$$\lambda = \langle \varphi_i^\alpha | \varphi_i^\beta \rangle \ \text{(for any } i).$$